The Astrophysical Journal, 838:95 (6pp), 2017 April 1 https://doi.org/10.3847/1538-4357/aa662c

Importance of Cross-redistribution in Scattering Polarization of Spectral Lines: The Cases of ^{3}P−^{3}S Triplets of Mg I and Ca I

M. Sampoorna and K. N. Nagendra
Indian Institute of Astrophysics, Koramangala, Bengaluru 560 034, India; sampoorna@iiap.res.in, knn@iiap.res.in
Received 2017 February 3; revised 2017 March 9; accepted 2017 March 9; published 2017 March 30

Abstract

Scattering on a multi-level atomic system has dominant contributions from resonance and Raman scattering. While initial and final levels are the same for resonance scattering, they are different for Raman scattering. The frequency redistribution for resonance scattering is described by the usual partial frequency redistribution functions of Hummer, while that for Raman scattering is described by cross-redistribution (XRD) function. In the present paper, we investigate the importance of XRD on linear polarization profiles of ^{3}P−^{3}S triplets of Mg I and Ca I formed in an isothermal one-dimensional atmosphere. We show that XRD produces significant effects on the linear polarization profiles when the wavelength separations between the line components of the multiplet are small, like in the cases of Mg I b and Ca I triplets.

Key words: line: profiles – polarization – radiative transfer – scattering – Sun: atmosphere

1. Introduction

Polarized line formation in multi-level atomic systems, including the so-called partial frequency redistribution (PRD) mechanism in line scattering, is a theoretically challenging problem. A self-consistent theory to solve this problem is under development (Casini et al. 2014; Stenflo 2015, 2016; Bommier 2016). A heuristic approach to this problem was presented in Sampoorna et al. (2013). Basically, they proposed an approximate approach to include polarization of radiation in the scalar multi-level PRD radiative transfer approach of Hubeny et al. (1983a, 1983b). They take into account frequency redistribution in both the resonance scattering (involving two levels) and Raman scattering (involving three levels). The frequency redistribution for a two-level atom is given by the well-known PRD functions of Hummer (1962), while that for a three-level atom is given by the cross-redistribution (XRD) function of Milkey et al. (1975; see also Hubeny 1982). The term "cross-redistribution" basically describes the frequency correlations that exist between two different transitions sharing a common upper level. The well-known examples where XRD is important are the L_α, L_β, and H_α lines of hydrogen (Hubeny & Lites 1995) and O I triplet at 130 nm (Miller-Ricci & Uitenbroek 2002; Anusha et al. 2014).

Sampoorna et al. (2013) applied their heuristic approach to the case of a five-level Ca II atom composed of the well-known H and K lines and the IR triplet lines. They showed that irrespective of the frequency redistribution mechanism, the Raman scattering contributes significantly to the linear polarization profiles of the IR triplet. However, the XRD does not play a significant role for these lines. This is because of the smaller damping widths of IR triplet lines and larger wavelength separations between the H and K resonance lines (in the blue part of the spectrum) and the IR triplet subordinate lines.

In the present paper, we apply the heuristic approach of Sampoorna et al. (2013) to compute the linear polarization profiles arising from ^{3}P−^{3}S triplets of Mg I and Ca I. For this purpose, we consider an isothermal planar atmosphere. The three strong lines at 5167, 5173, and 5184 Å belong to multiplet number 2 of Mg I, while the medium strong lines at 6103, 6122, and 6162 Å belong to multiplet number 3 of Ca I. These triplet lines are produced by the emission transitions $J = 1 \rightarrow 0$ (5167 or 6103 Å lines); $J = 1 \rightarrow 1$ (5173 or 6122 Å lines); and $J = 1 \rightarrow 2$ (5184 or 6162 Å lines; see Figure 1). Our aim is to investigate the importance of including XRD and Raman scattering in the computation of linear polarization profiles of these triplet systems. We chose these systems because of the relatively smaller wavelength separations between the line components. Also, these lines are strong to medium strong lines, so that the PRD and XRD effects could be important. Furthermore, Belluzzi & Trujillo Bueno (2011) have shown that in solar conditions (weak radiation field limit) the interference between the lower J-levels produces negligible effects on the linear polarization profiles of these lines. Therefore a multi-level atom approach is sufficient to describe these triplet systems.

Stenflo et al. (2000) present linear polarization observations of Mg I b and Ca I triplets obtained close to the solar limb. These observations show that the linear polarization amplitudes are nearly similar in all the three lines for both the Mg I b and Ca I triplets. Trujillo Bueno (1999, 2001) showed the necessity to include atomic polarization in the lower levels of these triplet systems, in order to interpret the previously mentioned observations. However, in the present paper we neglect the effects of lower level polarization. The numerical approach presented in Supriya et al. (2016), to include both the effects of PRD and lower level polarization in the problem of polarized line formation in a two-level atom, may be applied in future, to the cases of Mg I b and Ca I triplets. It is important to note that our present approach is not yet suited for a realistic modeling of linear polarization observations of solar Mg I b and Ca I triplets. This is because we make use of isothermal and not realistic model atmospheres for our studies (apart from neglecting lower level atomic polarization). We emphasize that the focus in the present paper is limited to assessing the importance of including XRD effects and Raman scattering when trying to model the linearly polarized line profiles of these triplet systems. A realistic modeling of the Mg I b and Ca I triplet lines is beyond the scope of the present work.

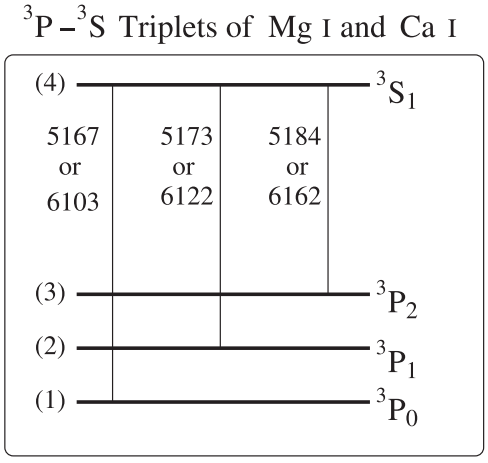

Figure 1. Level diagram corresponding to ^{3}P–^{3}S triplets of Mg I and Ca I. Energy levels are not drawn to the scale. Levels are labeled (1), (2), (3), and (4), in the increasing order of their energies. Electric dipole allowed transitions, along with their wavelengths (in Å), are marked by vertical solid lines connecting the levels.

The present paper is organized as follows. In Section 2 we briefly recall the governing equations and numerical method of solution presented in detail in Sampoorna et al. (2013). The model atoms and the model atmosphere are described in Section 3. The effects of XRD and Raman scattering on the linearly polarized line profiles for the ^{3}P–^{3}S triplets of Mg I and Ca I formed in an isothermal one-dimensional atmosphere are discussed in Section 4. Conclusions are presented in Section 5.

2. Polarized Line Formation in Multi-level Systems

In Sampoorna et al. (2013) the problem of polarized PRD line formation in multi-level atomic systems is solved by a two stage approach. In the first stage, the multi-level transfer problem for the unpolarized radiation is solved including both PRD and XRD in scattering. This scalar problem is solved by suitably generalizing the Multi-level Approximate Lambda Iteration (MALI-PRD) method of Paletou (1995). In the second stage, the polarized transfer equation for the multi-level system is solved using the number densities, line opacities, and line emission profile functions derived in the first stage. For this purpose, the polarized ALI method or the scattering expansion method is applied after suitable generalizations necessary to handle line-interlocking effects in a multi-level atom. For a review of these two methods, see Nagendra (2017; see also Nagendra 2003; Nagendra & Sampoorna 2009). In both the first and second stages, we use the angle-averaged PRD and XRD functions. In the absence of magnetic fields, the angle-dependent redistribution functions can be safely replaced by angle-averaged functions (see, e.g., Nagendra & Sampoorna 2011; Supriya et al. 2013; Sampoorna 2014).

The polarized transfer equation for the Stokes vector $\boldsymbol{I}_{ij}(x, \boldsymbol{\Omega}) = (I_{ij}, Q_{ij})^{\mathrm{T}}$ in a line that arises due to a transition between an upper level j and lower level i of a multi-level atom is given by[1]

$$\mu \frac{d\boldsymbol{I}_{ij}(x, \boldsymbol{\Omega})}{dz} = -[\chi_{ij}(x) + \chi_c][\boldsymbol{I}_{ij} - \boldsymbol{S}_{ji}], \tag{1}$$

[1] Reference direction for positive Q corresponds to the electric vector perpendicular to the limb.

where $\boldsymbol{\Omega}(\theta, \phi)$ represents the ray direction about the atmospheric normal, $\mu = \cos\theta$, x is the non-dimensional frequency in Doppler width units, $\chi_{ij}(x)$ is the line absorption coefficient, and χ_c is the background continuum absorption coefficient. The total polarized source vector $\boldsymbol{S}_{ji}(x, \boldsymbol{\Omega}) = (S^I_{ji}, S^Q_{ji})^{\mathrm{T}}$ is given by

$$\boldsymbol{S}_{ji}(x, \boldsymbol{\Omega}) = \frac{\chi_{ij}(x)\boldsymbol{S}^l_{ji}(x, \boldsymbol{\Omega}) + \chi_c \boldsymbol{S}^c_{ji}(x)}{\chi_{ij}(x) + \chi_c}. \tag{2}$$

The continuum source vector is assumed to be unpolarized and given by $\boldsymbol{S}^c_{ji}(x) = B_{\nu_{ij}}\boldsymbol{U}$, with $\boldsymbol{U} = (1, 0)^{\mathrm{T}}$ and $B_{\nu_{ij}}$ being the Planck function at the line center of the transition $i \rightarrow j$. Clearly we have as many transfer equations to be solved simultaneously as the number of allowed transitions in the multi-level atom. Different lines are coupled through the line source vector, which is given by

$$\boldsymbol{S}^l_{ji}(x, \boldsymbol{\Omega}) = \frac{A_{ji}}{P_j\,[n_i B_{ij} - n_j B_{ji}\rho_{ji}(x)]} \times \left\{ n_i B_{ij}\bar{\boldsymbol{J}}_{iji}(x, \boldsymbol{\Omega}) + \sum_{\substack{l\neq i,j \\ l<j}} n_l B_{lj}\bar{\boldsymbol{P}}_{lji}(x, \boldsymbol{\Omega}) + \left[n_i C_{ij} + \sum_{k\neq i,j} n_k (A_{kj} + C_{kj}) \right] \boldsymbol{U} \right\}, \tag{3}$$

where n's denote the number densities, A and B denote the Einstein coefficients, C denotes the inelastic collisional rates, P_j is the total rate out of a level j, and $\rho_{ji}(x)$ is the ratio of line emission profile function to the corresponding absorption profile function. The polarized resonance scattering integral is given by

$$\bar{\boldsymbol{J}}_{iji}(x, \boldsymbol{\Omega}) = \int_{-\infty}^{+\infty} \oint \frac{\boldsymbol{R}_{iji}(x, \boldsymbol{\Omega}, x', \boldsymbol{\Omega}')}{\varphi_{ij}(x)} \times \boldsymbol{I}_{ij}(x', \boldsymbol{\Omega}') \frac{d\Omega'}{4\pi} dx', \tag{4}$$

where $\varphi_{ij}(x)$ is the Voigt absorption profile for the $i \rightarrow j$ transition, and $\boldsymbol{R}_{iji}$ is the two-level atom redistribution matrix (Bommier 1997a, 1997b; see also Domke & Hubeny 1988). The polarized Raman scattering integral is given by

$$\bar{\boldsymbol{P}}_{lji}(x, \boldsymbol{\Omega}) = \int_{-\infty}^{+\infty} \oint \frac{\boldsymbol{R}_{lji}(x, \boldsymbol{\Omega}, x', \boldsymbol{\Omega}')}{\varphi_{ij}(x)} \times \boldsymbol{I}_{lj}(x', \boldsymbol{\Omega}') \frac{d\Omega'}{4\pi} dx'. \tag{5}$$

The Raman scattering redistribution matrix is denoted by $\boldsymbol{R}_{lji}$. Since the explicit form of this matrix is not available, we use the two-level atom expression itself, but with PRD functions (R_{II} and R_{III}) replaced by the corresponding generalized redistribution functions (P_{II} and P_{III}) of Hubeny (1982). Further, the K-multipole atomic polarizability factor W_K (with $K = 0,\ 2$) of resonance scattering is now replaced by the corresponding factor for Raman scattering (see Stenflo 1994; see also Landi Degl'Innocenti & Landolfi 2004). We note that

Table 1
Atomic Parameters Corresponding to the Four-level Mg I Atom Model

j	i	A_{ji} (s^{-1})	C_{ji} (s^{-1})	ν_{ji} (Hz)
2	1	Forbidden	4.80×10^4	6.01×10^{11}
3	1	Forbidden	2.88×10^4	1.82×10^{12}
4	1	1.13×10^7	4.10×10^4	5.80×10^{14}
3	2	Forbidden	8.65×10^4	1.22×10^{12}
4	2	3.37×10^7	8.23×10^4	5.79×10^{14}
4	3	5.61×10^7	9.22×10^4	5.78×10^{14}

Note. Statistical weights for the first four levels of Mg I are: $g_1 = 2$, $g_2 = 3$, $g_3 = 5$, and $g_4 = 3$.

Table 2
Atomic Parameters Corresponding to the Four-level Ca I Atom Model

j	i	A_{ji} (s^{-1})	C_{ji} (s^{-1})	ν_{ji} (Hz)
2	1	Forbidden	3.61×10^6	1.56×10^{12}
3	1	Forbidden	7.16×10^5	4.73×10^{12}
4	1	9.6×10^6	4.69×10^4	4.91×10^{14}
3	2	Forbidden	3.20×10^6	3.17×10^{12}
4	2	2.87×10^7	1.42×10^5	4.89×10^{14}
4	3	4.77×10^7	2.22×10^5	4.86×10^{14}

Note. Statistical weights for the first four levels of Ca I are $g_1 = 2$, $g_2 = 3$, $g_3 = 5$, and $g_4 = 3$.

the $P_{\rm II}$ function of Hubeny (1982) is identical to the XRD function derived by Milkey et al. (1975).

3. The Model Atoms and the Model Atmosphere

Figure 1 shows the level diagram for ^{3}P–^{3}S triplets of Mg I and Ca I. As shown in this figure, we consider the four-level Mg I and Ca I model atoms. Ca I has no nuclear spin, while 90% of the Mg I isotopes have zero nuclear spin. Here we neglect the contribution of 10% of the Mg I isotopes having a nuclear spin of 5/2. Furthermore, among 90% of even isotopes, 78.99% is in the form of ^{24}Mg and 11.01% in the form of ^{26}Mg. In the present paper we consider only the dominant even isotope—namely, ^{24}Mg.

Tables 1 and 2 list the main atomic parameters corresponding to the four-level ^{24}Mg and Ca I model atoms, respectively. The Einstein A coefficients corresponding to the Mg I b triplet are taken from Li & Qu (2015), and those for the Ca I triplet are obtained from National Institute of Standards and Technology (NIST) atomic spectra database (Kramida et al. 2015). The inelastic collision rates between the four levels of Mg I are obtained from the RH-code of Uitenbroek (2001) for a temperature of 5766 K, corresponding to a height of 910 km in the FALC (Fontenla et al. 1993) model atmosphere. For the Ca I atom case, these rates are again obtained from the RH-code for a temperature of 4410 K, corresponding to a height of 495 km in the FALC model atmosphere. We chose these heights, as they represent the mean values of line formation heights of the Mg I b and Ca I triplets, respectively. Levels 1, 2, and 3 are metastable levels, and hence are assumed to be infinitely sharp.

We consider an isothermal one-dimensional planar atmosphere. Bound-free transitions are neglected in our calculations. For the case of Mg I atom, the atmosphere is assumed to be at a temperature of 5766 K, while for Ca I atom it is at a temperature of 4410 K.

4. Polarized Line Profiles

For a ^{3}P–^{3}S triplet, we have scattering transitions of the type $J = 0, 1, 2 \rightarrow 1 \rightarrow 0, 1, 2$ (see Figure 1). This allows for nine different fluorescent combinations between the three initial and the three final states. The polarizability factors W_2 corresponding to these nine scattering transitions are listed in Table 3. Among these fluorescent combinations, three are due to resonance scattering and the other six are due to the Raman scattering. In other words, each line of the triplet gets one resonance and two Raman scattering contributions. In Sections 4.1 and 4.2, we discuss the effects of PRD and XRD on the linearly polarized line profiles of Mg I b and Ca I triplets, respectively.

Table 3
Polarizability Factor W_2 Corresponding to Nine Allowed Scattering Transitions in a ^{3}P–^{3}S Triplet

Radiative absorption/emission	$J = 1 \rightarrow 0$	$J = 1 \rightarrow 1$	$J = 1 \rightarrow 2$
$J = 0 \rightarrow 1$	1.00	−0.50	0.10
$J = 1 \rightarrow 1$	−0.50	0.25	−0.05
$J = 2 \rightarrow 1$	0.10	−0.05	0.01

4.1. The Case of Mg I b Triplet

Figure 2 shows a comparison of emergent (I/B, Q/I) profiles computed with and without Raman scattering and with CRD and PRD. Intensity profiles computed with CRD do not differ when Raman scattering is included or neglected (compare the dashed and dotted-dashed lines in the left panels of Figure 2). This is because for both of these cases $\rho_{ji}(x)$ is unity, since the line emission and absorption profiles are identical. On the other hand, corresponding intensity profiles computed with PRD differ considerably, particularly in the line wings (compare solid and dotted lines in the left panels of Figure 2). This is because $\rho_{ji}(x)$, which is now different from unity, differs for both of these cases (see Equation (11) of Sampoorna et al. 2013).

The Q/I profiles computed with and without Raman scattering differ considerably, irrespective of the CRD or PRD scattering mechanism. This is because of the very different polarizability factors for resonance and Raman scattering (see Table 3). Indeed, for the 5173 Å line, the Q/I computed with and without Raman scattering differ in sign. It is because the W_2 factor corresponding to resonance scattering in this line is positive, while those for both the Raman scattering terms W_2 are negative (see Table 3). As expected, the Q/I profiles computed with CRD are confined to the line core for all the three lines (see dashed and dotted-dashed lines). While the Q/I profiles computed for CRD with Raman scattering and PRD with Raman scattering nearly coincide in the line core (compare solid and dashed lines in the Q/I panels of Figure 2), they differ for those computed without Raman scattering (compare dotted and dotted-dashed lines). From Figure 2 it is clear that XRD effects (operating through Raman scattering) are significant for all the three lines, particularly in the wings. Indeed the large wing polarization is entirely due to XRD (compare solid and dotted lines).

Figure 3 shows the effect of background continuum absorption coefficient χ_c on the Q/I profiles of the Mg I b

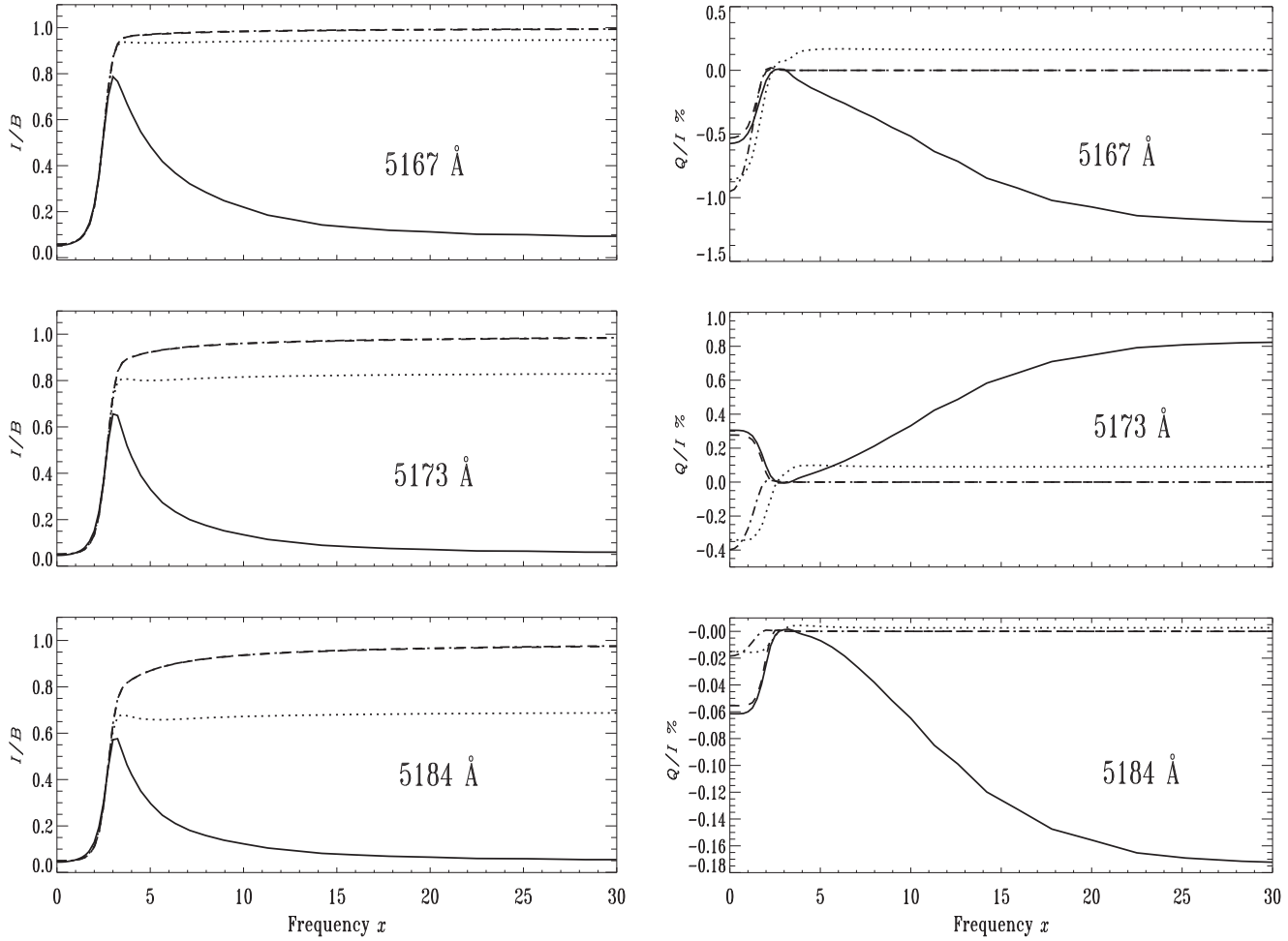

Figure 2. Normalized emergent I (left panels) and the degree of linear polarization Q/I profiles (right panels) of Mg I b triplet formed in an isothermal planar atmosphere at $T = 5766$ K. See Tables 1 and 3 for details on the atomic parameters. Line of sight is at $\mu = 0.047$. Background continuum absorption coefficient $\chi_c = 0$ and elastic collision rate $\Gamma_E = 0$. Different line types: solid (PRD with Raman scattering), dotted (PRD without Raman scattering), dashed (CRD with Raman scattering), and dotted-dashed (CRD without Raman scattering). In the left panels, dashed and dotted-dashed lines coincide.

triplet. The effects of PRD and XRD are taken into account when computing these profiles. As expected, finite background continuum absorption makes the wing polarization approach the unpolarized continuum value. And when it is not too large, the wing peak is formed due to XRD. Like in the standard two-level atom PRD case, the importance of XRD is also controlled by the value of χ_c.

Figure 4 shows the effect of elastic collisions on the Q/I profiles of the Mg I b triplet. Elastic collisions destroy the frequency correlation between incoming and outgoing photons via Γ_E and depolarize the scattered polarized radiation via $D^{(2)}$. The elastic collision rate $\Gamma_E = 2.939 \times 10^6$ s^{-1} is obtained from the RH-code for $T = 5766$ K corresponding to a height of 910 km in the FALC model atmosphere. Since we do not consider lower level polarization, the depolarizing collision rate $D^{(2)}$ actually corresponds to the upper level $J = 1$. From Equation (7.102) of Landi Degl'Innocenti & Landolfi (2004), we find that $D^{(2)} = 1.5 \times \Gamma_E$. Comparing solid and dotted lines in Figure 4, we see that as expected the elastic collisions decrease the Q/I throughout the line profile for all the three lines. The addition of the background continuum along with the elastic collisions has a similar effect of making the Q/I tend to zero polarization far in the wings. Thus we conclude that the XRD effect on Q/I profiles of Mg I b triplet lines do survive in the presence of small or moderate elastic collisions and a weak background continuum, and therefore should be accounted for when modeling these lines.

4.2. The Case of Ca I Triplet

For the case of Ca I triplet, we performed studies similar to those presented in Section 4.1 for the Mg I b triplet. The atomic parameters for the Ca I triplet are listed in Table 2. The planar atmosphere is chosen to be at $T = 4410$ K. We find that the shapes of the (I/B, Q/I) profiles of Ca I triplet are qualitatively similar to those presented in Figure 2 for the Mg I b triplet. Further, the XRD effects in the line wings are of similar nature. This is expected, because the Ca I triplet has a similar atomic configuration as the Mg I b triplet. Therefore we do not present the Q/I profiles of the Ca I triplet in graphical form. However, the unsigned amplitudes of Q/I in the line wings are somewhat smaller in the 6103, 6122, and 6162 Å lines as compared with the corresponding Mg I b lines. This is possibly due to the slightly larger separation between the line components of the Ca I triplet and also relatively larger values of inelastic collision rates (compare Tables 1 and 2).

As noted in Section 3, the Ca I triplet is formed at a height of about 495 km. In a FALC model atmosphere, the elastic collision rates at this height are $\Gamma_E = 1.56 \times 10^8$ s^{-1} for the

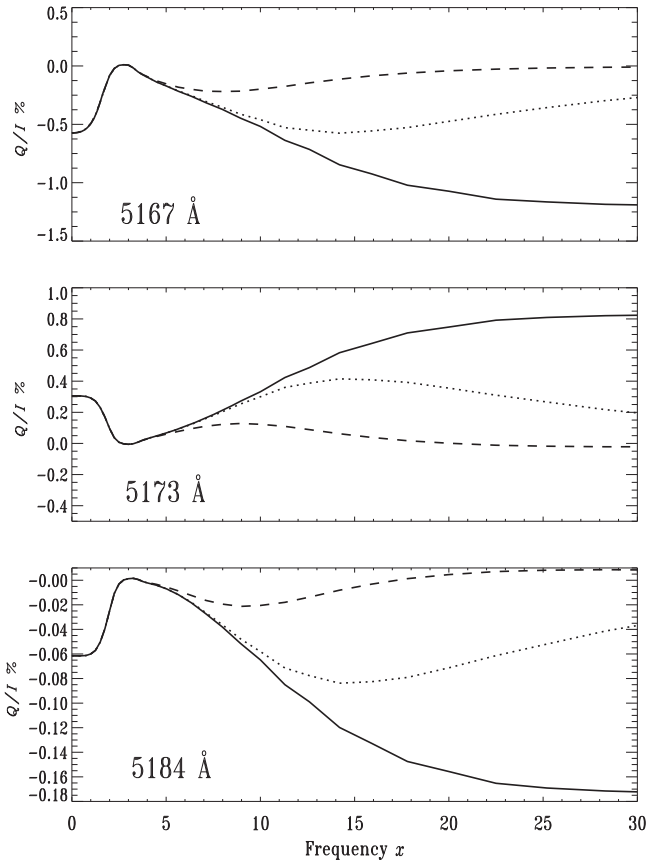

Figure 3. Effect of background continuum on Q/I profiles of the Mg I b triplet. Different line types are solid ($\chi_c = 0$ for all the three lines), dotted ($\chi_c = 10^{-8}$ for 5167 Å line, 2×10^{-8} for 5173 Å line, and 5×10^{-8} for 5184 Å line), and dashed ($\chi_c = 10^{-7}$ for 5167 Å line, 2×10^{-7} for 5173 Å line, and 5×10^{-7} for 5184 Å line). The line of sight is at $\mu = 0.047$. Other model parameters are the same as in Figure 2. The effects of both PRD and XRD in scattering are included.

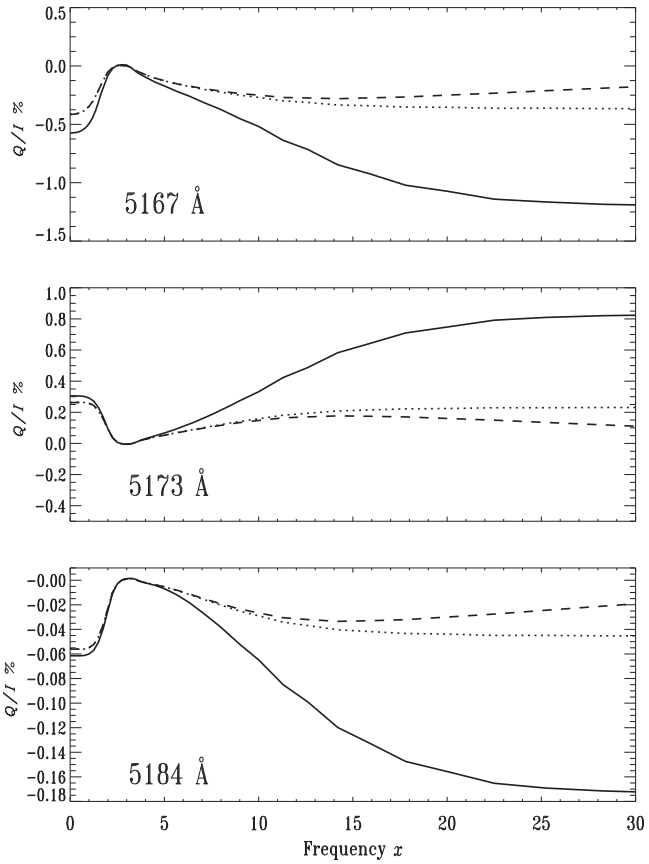

Figure 4. Effect of elastic collisions on Q/I profiles of the Mg I b triplet. Different line types are solid ($\Gamma_E = 0$ and $\chi_c = 0$), dotted ($\Gamma_E = 2.939 \times 10^6$ s^{-1} and $\chi_c = 0$), and dashed ($\Gamma_E = 2.939 \times 10^6$ s^{-1} and $\chi_c = 10^{-8}$ for 5167 Å line, 2×10^{-8} for 5173 Å line, and 5×10^{-8} for 5184 Å line). The line of sight is at $\mu = 0.047$. Other model parameters are the same as in Figure 2. The effects of both PRD and XRD in scattering are included.

6103 Å line, 1.19×10^8 s^{-1} for the 6122 Å line, and 1.31×10^8 s^{-1} for the 6162 Å line. Clearly these elastic collision rates are larger than the Einstein A coefficients corresponding to the Ca I triplet (see Table 2). Therefore the linear polarization profiles of the Ca I triplet that are computed including these elastic collision rates are strongly depolarized throughout the line profiles. Thus, unlike the case of the Mg I b triplet, the elastic collisions dominate over the XRD effects, leading to a vanishing linear polarization throughout the line profile.

5. Conclusions

It is well-known that the frequency redistribution in Raman scattering can be represented by the cross-redistribution (XRD) function of Milkey et al. (1975; see also Hubeny 1982). In the present paper we have studied the effects of this XRD on the linear polarization profiles of the ^{3}P–^{3}S triplet. To this end, we apply the heuristic approach of Sampoorna et al. (2013) to compute the linear polarization profiles produced in a four-level atom. We take the examples of Mg I b and Ca I triplet lines. For our studies, we have neglected the effects of lower level polarization.

We present the linear polarization profiles formed in an isothermal planar atmosphere. We show that the XRD effects are significant in the wings of Mg I b and Ca I triplet lines. This is in contrast to the case of the five-level Ca II model atom that was considered in Sampoorna et al. (2013). The reason for this lies in the fact that the wavelength separation between the multiplet component lines in the former case is smaller than between the H and K and the IR triplet lines of Ca II atom. Indeed, the use of traditional PRD function $R_{\rm II}$ of Hummer (1962) alone cannot fully account for the redistribution in the line wings of Mg I b and Ca I triplets, unlike the H and K lines of Ca II. What is required is in fact a combination of PRD functions of Hummer (1962) and the XRD function of Milkey et al. (1975). In particular, the XRD is necessary to model the linear polarization profiles of those multiplets that have closely spaced levels, resulting in increased line-interlocking effects.

In the presence of elastic collisions, the linear polarization of these triplets suffer a depolarization throughout the line profile. While the XRD effects survive in the case of Mg I b triplet lines, they vanish in the case of the Ca I triplet. This is because the Mg I b lines are formed at a height of 910 km, where the elastic collision rates are small, whereas the Ca I triplet lines are formed at 495 km, where the elastic collision rates are large compared with the radiative de-excitation rates. Thus we conclude that XRD effects need to be taken into account in the modeling of scattering polarization of multiplets such as Mg I b triplet lines, which are formed in the chromosphere where the elastic collision rates are smaller compared with the radiative de-excitation rates.

To test the validity of the present approach, it is necessary to apply this approach to model the actual linear polarization observations of solar Mg I b lines. For this, we need to include realistic one-dimensional solar model atmospheres, such as those given by Fontenla et al. (1993; see also Fontenla et al. 2009), in our present approach. Further, given that Mg I b lines are diagnostically important, there is a need to perform high-precision spectro-polarimetric observations of these lines, in particular to explore their spatial variations across the solar disk. Indeed our recent observations of Mg I b lines near the solar limb, obtained using ZIMPOL-III in 2016 September in collaboration with Dr. Michele Bianda of IRSOL, show that these lines do exhibit considerable spatial variations. We propose to apply our present approach of handling the cross-redistribution between the line components of a multiplet to model these new observations in the near future.

Computations are performed on a FORNAX (dual opteron 6220 with 8 cores and 3.0 GHz clock speed) computing facility at the Indian Institute of Astrophysics. Authors are grateful to J. O. Stenflo for useful comments that helped improve the manuscript.

References

Anusha, L. S., Nagendra, K. N., & Uitenbroek, H. 2014, ApJ, 794, 17
Belluzzi, L., & Trujillo Bueno, J. 2011, ApJ, 743, 3
Bommier, V. 1997a, A&A, 328, 706
Bommier, V. 1997b, A&A, 328, 726
Bommier, V. 2016, A&A, 591, A59
Casini, R., Landi Degl'Innocenti, M., Manso Sainz, R., Landi Degl'Innocenti, E., & Landolfi, M. 2014, ApJ, 791, 94
Domke, H., & Hubeny, I. 1988, ApJ, 334, 527
Fontenla, J. M., Avrett, E. H., & Loeser, R. 1993, ApJ, 406, 319
Fontenla, J. M., Curdt, W., Haberreiter, M., Harder, J., & Tian, H. 2009, ApJ, 707, 482
Hubeny, I. 1982, JQSRT, 27, 593
Hubeny, I., & Lites, B. W. 1995, ApJ, 455, 376
Hubeny, I., Oxenius, J., & Simonneau, E. 1983a, JQSRT, 29, 477
Hubeny, I., Oxenius, J., & Simonneau, E. 1983b, JQSRT, 29, 495
Hummer, D. G. 1962, MNRAS, 125, 21
Kramida, A., Ralchenko, Yu., Reader, J. & NIST ASD Team 2015, NIST Atomic Spectra Database (ver. 5.3), National Institute of Standards and Technology, Gaithersburg, MD, http://physics.nist.gov/asd
Landi Degl'Innocenti, E., & Landolfi, M. 2004, Polarization in Spectral Lines (Dordrecht: Kluwer)
Li, H., & Qu, Z. 2015, A&A, 573, A121
Milkey, R. W., Shine, R. A., & Mihalas, D. 1975, ApJ, 199, 718
Miller-Ricci, E., & Uitenbroek, H. 2002, ApJ, 566, 500
Nagendra, K. N. 2003, in ASP Conf. Ser. 288, Stellar Atmosphere Modeling, ed. I. Hubeny, D. Mihalas, & K. Werner (San Francisco, CA: ASP), 583
Nagendra, K. N. 2017, in ASP Conf. Ser. 1000, Solar Polarization Workshop 8, ed. L. Belluzzi et al. (San Francisco, CA: ASP), in press
Nagendra, K. N., & Sampoorna, M. 2009, in ASP Conf. Ser. 405, Solar Polarization 5, ed. S. V. Berdyugina, K. N. Nagendra, & R. Ramelli (San Francisco, CA: ASP), 261
Nagendra, K. N., & Sampoorna, M. 2011, A&A, 535, A88
Paletou, F. 1995, A&A, 302, 587
Sampoorna, M. 2014, in ASP Conf. Ser. 489, Solar Polarization 7, ed. K. N. Nagendra et al. (San Francisco, CA: ASP), 197
Sampoorna, M., Nagendra, K. N., & Stenflo, J. O. 2013, ApJ, 770, 92
Stenflo, J. O. 1994, Solar Magnetic Fields: Polarized Radiation Diagnostics (Dordrecht: Kluwer)
Stenflo, J. O. 2015, ApJ, 801, 70
Stenflo, J. O. 2016, arXiv:1610.09861
Stenflo, J. O., Keller, C. U., & Gandorfer, A. 2000, A&A, 355, 789
Supriya, H. D., Sampoorna, M., Nagendra, K. N., Stenflo, J. O., & Ravindra, B. 2016, ApJ, 828, 84
Supriya, H. D., Smitha, H. N., Nagendra, K. N., Ravindra, B., & Sampoorna, M. 2013, MNRAS, 429, 275
Trujillo Bueno, J. 1999, in ASSL 243, Solar Polarization, ed. K. N. Nagendra & J. O. Stenflo (Boston, MA: Kluwer), 73
Trujillo Bueno, J. 2001, in ASP Conf. Ser. 236, Advanced Solar Polarimetry: Theory, Observations and Instrumentation, ed. M. Sigwarth (San Francisco, CA: ASP), 161
Uitenbroek, H. 2001, ApJ, 557, 389